

# The Electrification of Thunderstorms and the Formation of Precipitation

J. Doyne Sartor

National Center for Atmospheric Research\*, Boulder, Colorado, USA

The problem of how thunderstorms become so highly electrified and whether the electricity in thunderstorms has anything to do with the growth of precipitation, especially in some of its unusual forms like hail, has been with science for a long time. Many controversies have developed over the explanation of the electrification. It now seems probable that the complexity of the questions and the severe difficulties encountered in making scientific measurements within thunderstorms have held up progress in this field. The acquisition of very high-speed high-storage capacity computers and high-resolution fast-response airborne instruments to cope with this complexity has made possible some recent and very significant progress in the understanding of these phenomena. We may conclude now that the bouncing, shattering and breaking of colliding particles in the developing electric field of cumulonimbus clouds will organize the electrical conditions in the cloud to produce the observed characteristics of thunderstorms.

An extremely rapid growth rate of the small droplets being formed continuously at cloud base is required in mature thunderstorms to insure that they are not carried through the cloud by the strong updraft without producing the observed heavy precipitation and hail. It has been shown that the electrical conditions inside thunderstorms can act to produce a greatly enhanced growth rate among these very small cloud droplets that otherwise would accrete only extremely slowly.

## *Introduction*

The thunderstorm is a well known and frequently experienced natural phenomenon for which there has been widely divergent opinions on its scientific explanation. It is agreed that the physical processes involved in the formation of precipitation and the generation of charge within it, run the entire gamut of the physics of all clouds. The cumulonimbus cloud, the classification type associated with a mature thunderstorm, is often referred to as a cloud factory. Almost every other classification of cloud can be identified with some portion of the cumulonimbus or as resulting from some physical process associated with it.

The number and complexity of the physical processes associated with the thunderstorm have made the quest for a unified theory to explain its growth and electrification extremely difficult and have fostered an almost complete dichotomy of the studies of cloud electrification and those of the growth of precipitation. Benjamin Franklin suggested a theory that cloud drops formed from water vapor originating from the sea would be charged with one sign and those from water vapor evaporating from moist soil would have the opposite sign. Consequently, when air of oceanic origin mixed with that of continental origin, as it frequently does in typical major weather disturbances, cloud drops from the separate sources

of water vapor, being of opposite sign, would be attracted to each other to form larger drops and finally rain. Franklin backed up his theory with observations of the electric field at his house to show that thunderstorms usually contained a net negative charge in the lower layers with a net positive charge above. The electrical polarity reported by Franklin is the same as that now normally observed in thunderstorms.

As early as 1879, Lord Rayleigh demonstrated that colliding water drops would normally bounce unless small opposite charges were added or an electric field was introduced into the region where the collisions were taking place. On the basis of these results, he commented that, "we should anticipate an explanation for the remarkable but hitherto mysterious connection between rain and electrical manifestations".

Recently, theoretical and laboratory studies [1—4] of the collision, accretion and bounce of cloud particles (liquid and solid) have added quantitative evidence that precipitation growth and the electrification processes in thunderstorms can be highly interactive. Theoretical models are not available yet for calculating the growth of precipitation interactively with the electrification processes. Models that consider each process independently require undesirable simplification in order not to exceed the capacity of the most modern computers. The formulation of a mathematical model of a thunderstorm is, at least, an expression of a complex hypothesis or interconnected hypotheses, that can be used to identify critical physical parameters for future field and laboratory studies. More-

\* The National Center for Atmospheric Research is sponsored by the National Science Foundation.

over, work with present day models, even when not solvable in their entirety, provides methods for seeking data compacting techniques and mechanisms for speeding up future calculations with the next generation of models and computers.

On the observational side of the problem, attempts to penetrate the interior of full grown thunderstorms are met with all the hostility of a fire-spitting dragon, hurling bolts of lightning, violent gusts of wind, and a fusillade of hail and freezing water at the intruder. One of Franklin's contemporaries was killed while using a kite to confirm Franklin's hypothesis that lightning was a large electrical discharge. A number of other investigators, including several in the last few years, have lost their lives in attempts to unravel the mysteries of thunderstorms. For the most part, we must be content to watch from the outside, observing the visual cloud boundary photographically, the accumulated water substance inside the cloud by radar, and the rain and hail deposited at the ground. The electrification is usually sensed indirectly with instruments at the ground or carried aloft by aircraft flying mostly outside the cloud. Occasionally, penetrations of mature thunderstorms are made with instrumented aircraft. Even with repeated traverses, the data obtained are representative of a very small portion of the storm over a very limited period of time. At best, the data cover an unknown period in the life cycle of a storm and the probability of encountering the central precipitation and electrification growth regions of a large cloud is small.

Why is it important, other than to satisfy natural curiosity, to understand how thunderstorms develop? The atmosphere frequently is referred to as a heat engine; moving heat, moisture and momentum from lower latitudes poleward. Cloud motions, particularly those of the cumulonimbus, process the heat, moisture and momentum and carry the energy thus obtained upward from the tropical oceans into the upper levels of the atmosphere where it helps fuel the global circulation and is transported poleward by it. Without clouds and the precipitation from them to remove the pollutants from the atmosphere, the smaller particulates would continue to accumulate there. On the other hand, if it were not for the extrinsic particulate material in the atmosphere to act as nuclei for the millions of cloud drops necessary for the formation of each of a vast number of raindrops, clouds, as we know them, would never form. Through the nucleation properties of particulates, man has a demonstrated capability to modify clouds to some degree. The full extent of the modification efforts has yet to be determined, especially over an entire region. Clearly, we must understand cloud processes if we are to continue to try to alter them or to use them to help us keep the atmosphere clean, to place rain or snow where we need it, and to alleviate the destruction sometimes caused by the most severe storms.

#### *Theoretical Models as Guides to Observation*

Piecing the direct observations together with the indirect measurements and some laboratory studies on the nucleation and growth of solid and liquid hydrometeors, we can now present a crude universal model of a thunderstorm. Based on this model, and the

questions it leaves unanswered, we can plan an attack on the problem with existing technology that concentrates on the developing, less chaotic, but more informative stages; avoiding wherever possible, a direct confrontation with the chaotic mature stage. In doing this, we make the tacit assumption that the information we obtain from the developing stages will lead naturally and directly to an understanding of the mature stage and its sometimes violent consequences. At most temperatures above  $-40^{\circ}\text{C}$ , cloud droplets form in the atmosphere as a consequence of the diffusion of water vapor onto condensation nuclei when moist air is cooled to saturation by adiabatic expansion. Ice crystals appear as the air continues to cool by expansion to temperatures usually considerably below  $0^{\circ}\text{C}$ , when nuclei with the particular ability to initiate freezing of the supercooled droplets are present.

In the free atmosphere, the adiabatic expansion results from the lifting of the air by its movement over terrain of increasing height, over air of greater density, in response to the larger scale circulation, or as a consequence of thermodynamic instability. The larger scale circulation with a characteristic wave-length of one hundred to several thousand kilometers can encourage or inhibit the upward motion of the air on the more local scales associated with thunderstorms. Upward vertical air motion is encouraged when the horizontal motion of the air undergoes convergence in the lower levels and divergence in the upper levels, and warm air is advected into the lower levels or cold air into the upper levels or both. Upward moving air is inhibited to the degree that any of these characteristics of larger scale circulation act in the reverse sense. Calculations of the vertical motion created by the larger scale circulations give values in the  $\text{cm sec}^{-1}$  range, while measurements of the order of  $\text{m sec}^{-1}$  are commonly obtained. Thunderstorms contain updrafts and downdrafts exceeding  $10 \text{ m sec}^{-1}$ .

The calculations of vertical motion based on observations of the larger scale circulation are of necessity based on spatially averaged data and therefore represent a net vertical component that is completely unrealistic in magnitude for the thunderstorm scale.

This averaged circulation (determined by the present network of observation stations and the grid scale of current prediction models) is nevertheless extremely useful in specifying the areas where thunderstorms can and probably will appear. The scales of motion associated with convective clouds and thunderstorms, one to ten kilometers, are preferred by the atmosphere as more efficient for the transport of heat, moisture and momentum upward.

The thermodynamics of the local convective process applied to a cumulonimbus cloud is schematically illustrated in Fig. 1, where the horizontal scale is temperature increasing to the right and the vertical scale represents the height (an inverse function of pressure). The thin solid line represents the dry adiabatic lapse rate as indicated in the diagram. The heavy line, with frequent changes of slope, indicates an hypothetical temperature sounding of the ambient atmosphere. The dashed line to the left of the other curves (a line of constant water vapor mixing ratio through the saturation point of the temperature sounding) intersects the surface at the surface dewpoint

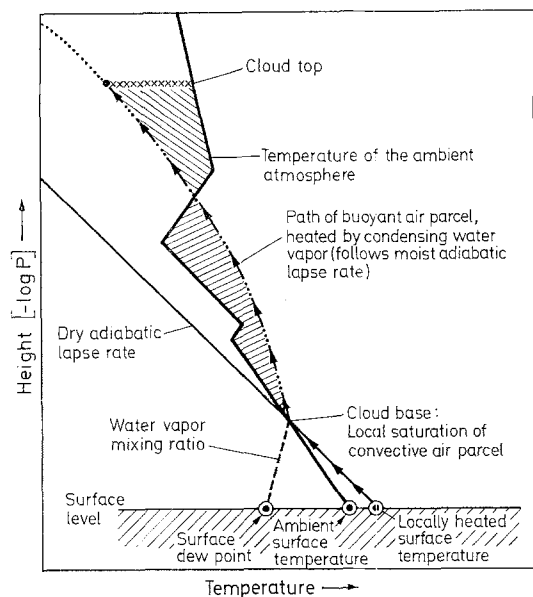


Fig. 1. Schematic diagram illustrating the thermodynamics of local convective processes

temperature. If by differences in the heating characteristics of an inhomogeneous surface, or due to small scale circulation perturbations, the surface temperature in one location rises to that indicated on the diagram as the "locally heated surface temperature", the temperature lapse rate in the lowest layers can approach the dry adiabatic lapse rate as shown. Any further perturbation in the temperature or upward motion, however small, will initiate a convective parcel of air that accelerates upwards; its temperature change following the dry adiabatic lapse rate until saturation is reached at a point where its temperature is equal to the dewpoint temperature. At this point, determined by the intersection of the ambient temperature curve with the dashed (mixing ratio) line extending upward from the surface dewpoint temperature, the cloud begins to form by water vapor diffusion to condensation nuclei always present in the atmosphere. The height of this point above the surface is observed with a high degree of reliability to be the altitude of the base of the cloud.

As soon as cloud droplets start to form, the parcel of upward moving air is heated by the release of the latent heat of condensation and the temperature increases more rapidly with height following the curved line which is depicted in Fig. 1 by the upward pointing arrows as the path of the buoyant air parcel. The shape of this path is referred to as the moist adiabatic lapse rate for saturated air. As the air continues to rise it will eventually cross the ambient temperature curve (heavy solid line) again. The area between the moist adiabat and the ambient temperature curve below this cross-over point is representative of the energy added to the parcel of air in the cloud. Above the cross-over point the temperature of the upward moving air falls below the ambient temperature and the parcel of air starts to lose the energy gained below this level. When the energy (represented by the area between the two curves) lost above is equal to that gained below the cross-over point on the diagram, the cloud will have reached its ultimate height. The cloud

top is indicated by the line of *x*'s between the moist adiabat and the temperature sounding of the ambient atmosphere.

The above schematic representation of cloud thermodynamics can occur in the real atmosphere only when there is no mixing of the cloud air with surrounding ambient atmosphere. This can never be true in general. However, it may closely approximate the conditions in the core of the updraft of large cumulus and cumulonimbus clouds. In the tropics and in the continental United States, it is not unusual for the tops of cumulonimbus clouds to exceed 12 to 15 km. The change of temperature and pressure with height of the rising parcel of air (shown in Fig. 1 by the line of arrows) provides us with values of cloud base and top that substantially agree with observations, but do not give us quantitative values of the fundamental variable, the vertical velocity of the rising air in a cloud. For example, if  $T'$  is the Kelvin temperature of the rising parcel of cloud air and  $T$ , the Kelvin temperature of the displaced ambient air at the same level, the vertical acceleration of the cloud air due to its buoyancy is

$$\frac{dU_z}{dt} = g \left( \frac{T' - T}{T} \right). \quad (1)$$

Integrating this equation using parcel and ambient air temperatures from thermodynamic analyses like that illustrated in Fig. 1, does not give realistic values for the vertical velocity,  $U_z$ . These unrealistic values can be adjusted by including considerations of the drag forces on the rising parcel of air and the dilution of the warm moist cloud air with the cooler drier air to reduce  $T'$ . When we attempt to do this we usually find that, although we can make suitable empirical adjustments for specific situations, we have not found a formulation that is generally applicable. The difficulty may be largely due to the restrictions placed on fully three dimensional models of convective clouds by the speed and storage capacities of present day computers, forcing us to consider one and two dimensional models that specify arbitrarily the cloud shape, volume or horizontal extent.

The vertical velocity of the air in clouds must be obtained since all physical parameters of importance in cloud development depend on it and it is needed to introduce time variations into the calculations of the physical processes leading to precipitation growth and thunderstorm electrification. But as we have just stated, it is difficult to obtain the vertical velocity from the thermodynamics of the atmosphere and, as discussed earlier in this section, calculations from the equations of motion for the large scale circulation give quantitative values orders of magnitude too small. This situation has made the quest for a good technique of measuring the vertical velocity in clouds one of primary concern.

#### *Microphysics of Precipitation and Electrification*

Clouds develop rain, snow or hail mainly by two processes. At temperatures above  $-40^\circ\text{C}$ , the growth normally starts by the diffusion of water vapor onto airborne particulates to form small liquid droplets and possibly ice crystals at the colder temperatures. Below  $-40^\circ\text{C}$ , the homogeneous freezing nucleation temperature, ice crystals could form directly from the vapor,

or immediately after the formation of a cloud droplet. While the growth by diffusion continues, the growth by accretion between the larger faster falling cloud drops or ice particles and the smaller slower falling ones begins slowly at first, but eventually becomes the dominant mechanism in the more vigorous convective clouds like the cumulonimbus.

The equation for the diffusion growth is the better understood of the two processes. We know, for example, that under the same temperature and moisture conditions, ice crystals will grow on the order of 100 times faster than coexisting supercooled droplets. The diffusion growth of cloud particles follows the classical laws of mass and heat flow and includes the thermodynamics of condensation and the freezing of water solutions and the crystalline growth habits of ice. The calculations result in a complex quantitative interaction among all these contributions. In addition, there are laboratory studies indicating that under strong electrical fields, or with highly charged particles, diffusion growth can be significantly altered, but the conditions cannot be related quantitatively to natural conditions in the free atmosphere at this time.

The situation is quite different for the growth of precipitation by the coalescence of cloud droplets, and the accretion of ice particles and cloud droplets by larger ice particles. Here, some of the physical processes are simpler, but the total way they interact is difficult to describe analytically. We know from observations that the time required for precipitation growth is too short to be explained by diffusion growth alone. It has been a difficult proposition to explain the rapid growth by coalescence and accretion also without evoking artificially large drops or electric charges and fields that are not normally observed in the beginning stages of cloud development. The fact is that values of some of the parameters, that must be considered quantitatively, are not well known. The better quantitative information must be obtained from extensive laboratory studies and from observations in the actual atmosphere. It is known, however, that the rate of interaction of particles relative to one another, which controls their growth, is strongly affected by electric charges and fields and that the processes of particle interaction have a strong, if not overriding, influence on the development of thunderstorm electrification. For this reason, we will go into the microphysical interaction of colliding, accreting and bouncing particles in some detail.

It is common observation by both laymen and scientists, that the first gush of rain frequently follows shortly after the first lightning stroke. From the scientists' viewpoint the observations that strong electrification in a cloud follows very quickly after the initial appearances of ice particles, are even better substantiated. It is also true that, in most cases, there are both liquid and ice particles coexisting in the same volume of an active thunderstorm. Occasionally, thunder and lightning occur with a very heavy snowfall at air temperatures near  $0^{\circ}\text{C}$  from clouds that apparently are glaciated completely, and there are a number of reported instances of lightning in clouds that probably contained only liquid water drops. Thunderstorm theory should allow for both of these possibilities, even if they are rare occurrences.

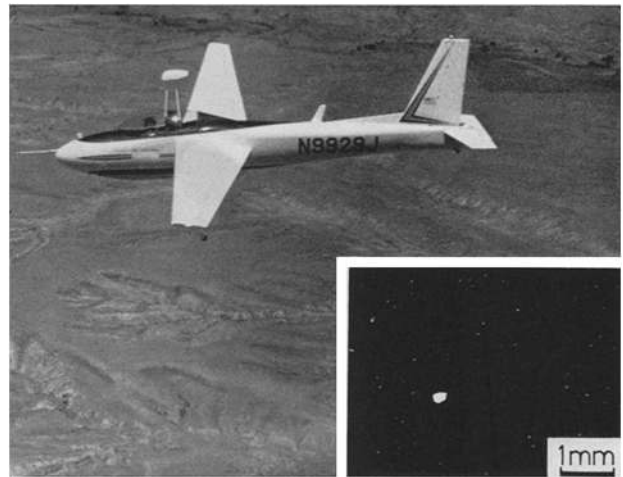


Fig. 2. Close up of The Explorer sailplane in flight and *in situ* photographs from sailplane of coexisting supercooled cloud drops and a rimed ice particle at  $-22^{\circ}\text{C}$  (insert)

In our own work with an instrumented sailplane, we have made *in situ* photographs of millimeter ice particles and micron size supercooled cloud droplets, as illustrated in the lower right hand corner insert in Fig. 2. On sustained flights in the updraft of summer cumulus clouds the sailplane encountered only supercooled droplets less than  $12\ \mu\text{m}$  radius until suddenly rimed ice crystals or graupel appeared. Rimed ice crystals and graupel can occur only as the result of the collection by a much larger ice particle of a great number of supercooled droplets that freeze on contact. These observations fit our present understanding of cloud droplet and ice crystal nucleation and growth. Ice nuclei that are active at temperatures below  $-10$  to  $-15^{\circ}\text{C}$  are rare, but once a supercooled droplet around  $-10^{\circ}\text{C}$  encounters one of these rare nuclei and freezes, it will grow very rapidly by diffusion (over 100 times as fast as the neighboring droplets) due to the low saturation vapor pressure of ice. After this rapid initial diffusion growth, the ice crystal will be large enough to fall rapidly with respect to the supercooled cloud droplets, collecting them and causing them to freeze upon contact. Numerous other observations have connected the sudden appearance of strong electrification with the first observations of the ice phase in clouds.

We find that the production of precipitation by the rimed ice or graupel process is quite general in the mountainous and high plains area of Colorado. Evidently, the first precipitation that falls to the ground as rain or hail throughout much of the precipitation life history of convective clouds in this region, starts its fall from altitudes above the  $0^{\circ}\text{C}$  isotherm as graupel. Similar observations have been made by Workman and Reynolds [5], and Reynolds, Brook, and Gourley [6] in New Mexico and by numerous other scientists studying continental clouds of the western USA.

Using these observations as a guide for simplifying the highly complex physical processes involved, we can write equations for the accretion growth of precipitation and the electrification of thunderstorms as a consequence of the same processes. Mathematically, then, we will specify that there are two distributions of

particles; one for the larger particles, 100  $\mu\text{m}$  to 0.5 cm radius and larger, and the other for the cloud droplets, 1 to 20  $\mu\text{m}$  radius. The larger particles are too scarce and too widely dispersed to interact significantly among themselves and the cloud droplets are so small that the probability of them colliding with each other sufficiently often to grow significantly is negligible. This situation would be true to a high order of accuracy of the distributions of supercooled cloud droplets and rimed ice particles depicted in lower insert of Fig. 2; a configuration that is common in developing cumulus clouds in Colorado.

The particle interaction processes are expressed in Eqs. (2a) and (2b). The summation or integration operations will not be specifically identified, since the choice will depend on the form of the size distributions and on the characteristics of the other parameters. Eqs. (2a) and (2b) are written one above the other and the corresponding factors arranged so that their similarity can be identified readily for demonstrating the close relationship between the rate of growth of precipitation, Eq. (2a), and the rate of charging of the particles per unit volume, Eq. (2b).

The growth of precipitation results from the collisions between the larger particles and the smaller ones that result in accretion or coalescence. The charging occurs when the particles bounce or otherwise separate after colliding. The mass growth rate of the precipitation per unit volume and the charging rate per unit volume are respectively,

$$\frac{\delta m}{\delta t} = \mathbf{S} \mathbf{S} n_R n_r [\pi(R+r)^2 (V_R - V_r) E_c E_a] \cdot (4/3 \pi \rho_r r^3) \delta r \delta R \quad (2a)$$

and

$$\frac{\delta Q}{\delta t} = \mathbf{S} \mathbf{S} n_R n_r [\pi(R+r)^2 (V_R - V_r) E_c (1 - E_a)] \cdot \left( \Psi t + \Phi \int_0^t F dt \right) \delta r \delta R. \quad (2b)$$

In the equations, the probability that a small droplet in the path of a larger particle will actually collide with it is specified by  $E_c$ , the collision efficiency, and the probability that it will adhere to the larger particle is given by  $E_a$ , the accretion efficiency. Both of these probabilities are affected by charges on the particles and by the ambient electric field in which they collide. We let  $R$  be the radius of a larger ice particle and  $r$  the radius of a smaller cloud particle, while  $n_R$  and  $n_r$  and  $V_R$  and  $V_r$  are respectively their number densities per unit volume and their fall velocities.  $F$  is the ambient electric field, and  $\Psi$  and  $\Phi$  are charge transfer functions to be specified later in the discussion.

The expression in the square brackets in Eq. (2a) is commonly referred to as the accretion "kernel" due to its being considered as an "integration kernel" when seeking analytical solutions to this integrodifferential equation. Eq. (2b) contains a similar expression in square brackets; it corresponds to the accretion kernel, but since it contains  $(1 - E_a)$  instead of  $E_a$  it represents a separation kernel. The product of  $n_R n_r$  and the accretion kernel gives the number of droplets collected per unit volume per second. To get the rate of change of mass of the larger particles per unit volume, this product (the number of collections per

unit volume) is multiplied by the mass of each accreted smaller drop.

The equation for the rate of separation of charge due to the particle collision and bounce, Eq. (2b), and the precipitation growth rate equation, Eq. (2a), have a parallel structure throughout. The product of the number concentrations of the large and small particles,  $n_R n_r$ , appears first in both. Instead of the accretion kernel of (2a), Eq. (2b) contains the separation kernel and the charge transfer functions factor,

$$\left( \Psi t + \Phi \int_0^t F dt \right),$$

is substituted for the accreted mass term,  $(4/3 \pi \rho_r r^3)$ . Within the function  $\Psi$  can be included all the charging processes that are independent of the electric field, while the function  $\Phi$  includes those that are due to induction charging of colliding, accreting and bouncing particles in the electric field of the atmosphere. Convective rearrangement of the normal charge distribution in the free atmosphere and other charging processes occurring in the very early stages of cloud development can be accounted for by an appropriate value of the initial electric field when the primary concern is the electrification of thunderstorms. The electric field of the free atmosphere is close to 1 V  $\text{cm}^{-1}$  at the surface decreasing exponentially with height. Electric fields of over 5 000 V  $\text{cm}^{-1}$  have been observed inside active thunderstorms.

Our theoretical investigation of Eq. (2b) shows that most of the contribution to the growth of electrification in thunderstorms can be accounted for by the physical process of the interaction of the larger particles with the much smaller particles, using the fair weather electric field as the initial field, thus Eq. (2b) is, in fact, a reasonably good approximation to the rate of separation of charge in a thunderstorm. Electric fields like those observed in thunderstorms are obtained readily with particle distributions observed in active thunderstorms by Jones [7].

In Eq. (2a), the assumption that all of the interactions are between the much larger particles and the very small ones is not a good approximation until the late stages of the precipitation growth have been reached. In the early stages of cloud development, all droplets are small and must collide and combine with each other in order to grow sufficiently rapidly to explain the observations. In this case, equations similar to Eq. (2a) can be used, but now  $n_R$  and  $n_r$  are the concentration of the larger and the smaller of each interacting drop pair, and  $R$  and  $r$  are allowed to vary over the full range of droplet sizes in a continuous or piecewise continuous fashion. Analytical solutions to this generalized formulation are available only for certain types of expressions for the accretion kernel, namely of the form,  $A + B(x + y) + Cxy$ , where  $x$  and  $y$  are functions of the variables in the kernel and  $A$ ,  $B$ , and  $C$  are constants.

The generalized Eq. (2a) can be solved with numerical methods also, but these can be very time consuming and tedious, and serious problems will develop if the droplet distributions fluctuate with the changes in space or time. These calculations assume an initially random distribution of cloud and precipitation particles in space throughout the cloud, with each parcel of a cloud being statistically the same as all other parcels of the same volume, at the same time or height within the cloud.

#### *Observations and Calculations Applied to Theory*

It is inherent in calculations using Eqs. (2a) and (2b) and equations of similar form expressing the results of cloud particle interaction, that the particle size

distributions change monotonically to produce larger drops out of an initial distribution of smaller drops. The capability to make observations in actual clouds of vertical motion and other vital microphysical parameters on the time and space scales required, has been acquired within the past year. The variability observed in the cloud drop distributions just tens of meters apart in growing cumulus clouds is considerable. The rapid appearance of mm size graupel or rimed ice crystals at temperatures several degrees below 0 °C, with dimensions orders of magnitude larger than the cloud drops, obviates the need for the cloud drops of dimensions 1 to 12 μm (the size range we frequently observe in continental clouds) to grow only among themselves. On the other hand, heavy icing observed occasionally on aircraft when penetrating the active regions of thunderclouds and the occurrence of large hail requires that many larger supercooled drops (100 μm or greater) be present in the clouds. These large supercooled drops could result from recycled melted graupel or ice crystals, but it is more likely that they grow from interactions among the cloud droplets. We do know that rain and possibly lightning occur in clouds containing only the liquid phase. For these reasons a considerable effort has gone into studies of cloud droplet collision and coalescence.

Using the earlier descriptions of significant events in the life history of the growing cumulonimbus cloud and its electrification, together with the formulation in Eqs. (2a) and (2b), we can establish which observations and calculations are of primary importance for understanding the interaction of precipitation and electrification in thunderstorms. The observations and calculations of principal concern in the order of their importance are:

A. Measurements of the horizontal and vertical profiles of the vertical velocity in clouds are required simultaneously with observations of the temperature and humidity variations with height on the cumulus and cumulonimbus cloud scale.

B. High resolution, fast response measurements of cloud particle size and charge distribution must be made as functions of temperature, the vertical motion of the air and ambient electric field. These measurements must be made on time and space scales that are small compared to the dimensions of the cloud and are required for both cloud electrification and precipitation growth.

C. The number density of condensation and freezing nuclei should be measured continuously in the air entering the base of the clouds with automatic fast time response instruments. Initial droplet distribution data followed by changing distributions in the updraft would be acceptable substitutes for nuclei observations for the immediate future.

D. The collision efficiency,  $E_c$ , and the accretion efficiency,  $E_a$ , which are known to be functions of drop size, charge and electric field must be measured in the laboratory to check theoretical calculations already well advanced.

E. As any of the measurements or calculations itemized above are obtained, they must be used in the computer models of precipitation growth and electrification, containing component formulations like those of Eqs. (2a) and (2b), to test the applicability of the models,

find ways to improve them and to suggest further measurements. The models are considered in this context as complex hypotheses to be modified to fit new observational information and improved scientific understanding.

#### *State of Progress in Thunderstorm Research*

We will now discuss observations and calculations distilled from a great number of past and continuing research efforts in an attempt to inform the reader of the present state of scientific understanding and current capability for exploring the areas of primary concern just listed. There are presently three methods of observing the vertical velocity in developing cumulus clouds; *doppler radar*, *dropsondes* and *aircraft*.

Doppler radar senses the absolute motion of the cloud and precipitation particles and the vertical motion is obtained by subtracting their fall velocity with respect to air, assuming that in the cloud their fall velocity is the same as calculated theoretically or observed in the laboratory. It is necessary to know the charges on the cloud particles and the electric field at the same place in order to be sure. Doppler radar provides us with an extremely valuable tool. Minor drawbacks are that it gives averaged velocities over considerable volumes at times spaced further apart than we would sometimes like. Sondes dropped into the top of major thunderstorms to fall with a high speed are being used to obtain the vertical velocity in a manner similar to that used to obtain the true air speed on aircraft. Although valuable data have and are being obtained, they are considered as still somewhat developmental because of the difficulty in obtaining other vital types of information with them.

Aircraft are the most frequently used and the most versatile tools for thunderstorm research due to their maneuverability and instrument carrying capacity. Most of the types of data required can be obtained, sometimes with difficulty because of the pollution and disturbance caused by the craft itself. The major problem is finding the vital updraft in the storms and making observations of the vertical motion that do not require extremely elaborate and sophisticated engineering such as inertial platforms to permit later corrections for aircraft attitude and power settings.

Within the past year we have begun to obtain an extremely valuable combination of cloud data using a high-performance sailplane (see Fig. 2) instrumented to obtain vertical velocity, particle size and distributions of supercooled droplets and ice crystals, along with the necessary parameters to describe the physical environment in clouds. Vertical velocities with an accuracy of 0.2 to 0.5 m/sec, are obtained this way from a simple equation of motion for the sailplane. Its emergence as a valuable research tool is the result of recent developments in solid state electronics, small volume light weight long life batteries, and small light weight automatic cloud particle probes. Its most valuable feature for cloud physics research appears when its high glide ratio is combined with the skills of an experienced pilot to seek out and find the core of an updraft inside or outside clouds. The pilot can maneuver to obtain the horizontal profiles of the updraft or remain in its core while the other parameters of vital significance are being obtained with

sensors operating automatically. A sailplane, carrying a pilot and an observer, leaves not a great deal of weight for instrumentation, especially recorders. Therefore, the information from the sensors for the most part is relayed continuously to the ground by telemetry and displayed in real time on chart recorders and oscilloscopes and recorded for later analysis on magnetic tape. The present operational system allows for automatic digitalizing of the data and transfer to the computer where the data can be processed for use in models of precipitation growth containing factors like those in Eqs. (2a) and (2b).

Although a great deal of data is obtained in a very short time with the extremely desirable feature of having fast response and high repetition rate, there will not be enough data until the end of this summer to draw very many firm conclusions concerning thunderstorm precipitation and electrification development.

Fig. 3a—c are selected one-minute samples of three of the computer-processed parameters obtained with The Explorer sailplane flown by the Cloud Physics Program research team of the National Center for Atmospheric Research on 15 July 1971 in the updraft of a cumulus cloud in Northeastern Colorado as part of a large scale field research effort on the nature of severe hailstorms. In each figure, time increases from left to right with the time of the start and end of each one-minute sample printed out according to the 24 hour clock in Greenwich Time (GMT). The vertical scales are divided into three sections, with the vertical speed of the air at the top (ranging from  $-10$  m/sec to  $10$  m/sec); the total liquid water content (LWC) of the cloud drops (grams meter $^{-3}$ ) in the center. The cloud droplet number density data in each of the ten drop-size channels given in Table 1 is summed over each 1/2 sec interval, with each of the data points connected by a straight line in the figures by a computer plotting routine. The drop-size intervals represented by the numbers attached to each of these lines in the bottom portion of each figure are the drop-size channel numbers in Table 1. Temperature, altitude and true air speed are plotted also, but are not included in these illustrations. The altitude covered a climb of several hundred meters with a mean altitude of about  $4.2$  km. The temperature was approximately  $8^{\circ}\text{C}$  and the true air speed of the sailplane close to  $50$  m/sec.

The one-minute interval during which the sailplane, moving upward with the updraft, entered the base of the cloud is shown in Fig. 3a. The data sample in Fig. 3b was taken in the interior of the cloud and that shown in Fig. 3c was recorded as the sailplane left the top of the cloud. Note that there is a rough correspondence between the up and down drafts and the droplet distributions with a time lag of several seconds, indicating that the evaporation of the cloud droplets is very rapid over a vertical distance of possibly not more than a few tens of meters. The droplet distributions are observed at the tip of the boom extending horizontally from the nose. Fig. 2 is a close-up photograph of The Explorer sailplane in flight with an insert showing a sample *in situ* photograph of co-existing cooled cloud droplets and graupel ice particles. The wing shaped object, about a meter above the canopy of the sailplane, is the light trap and light reflection source for photographing cloud droplets

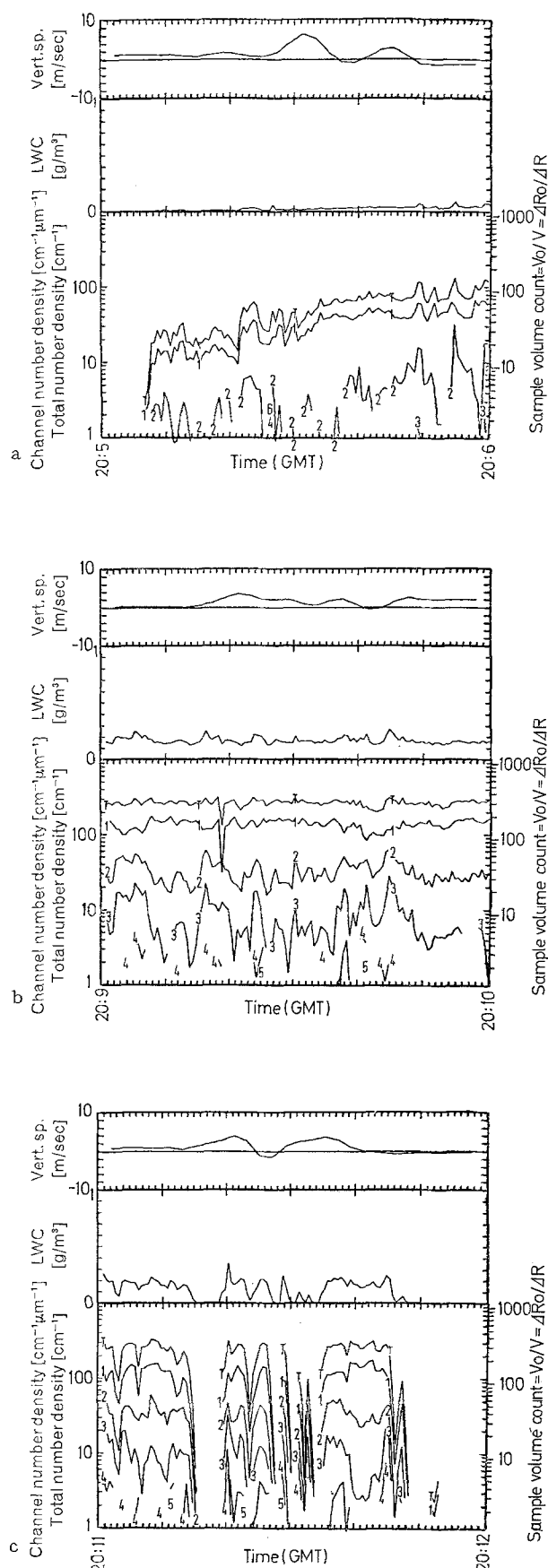


Fig. 3a—c. One-minute samples of computer-analyzed data from sailplane in cumulus cloud, 15 July 1971. a) 2005 to 2006 GMT; b) 2009 to 2010 GMT; c) 2011 to 2012 GMT

Table 1. Channel number corresponding to drop radius interval of The Explorer sailplane cloud droplet probe

Channel number	Radius interval [ $\mu\text{m}$ ]
1	4.0—5.5
2	5.5—7.0
3	7.0—8.5
4	8.5—10.0
5	10.0—11.5
6	11.5—13.0
7	13.0—16.0
8	16.0—19.0
9	19.0—22.0
10	>22.0

and ice particle images in a volume approximately the size of a 35 mm slide roughly half-way between the small wing and the canopy. Photographing the cloud particles this way results in an undisturbed sample. This instrument is described in a paper by Cannon [8].

The automatic cloud droplet probe in the long slender nose boom is described in a paper by Abbott, Dye, and Sartor [9].

The observation of condensation and freezing nuclei appropriate for atmospheric processes is very difficult due to the necessity for artificially producing supersaturation for the activation of the condensation nuclei, and supersaturation followed by cooling for freezing nuclei. The rates of cooling, and the pressure in the atmosphere, change and fluctuate in ways that are virtually impossible to reproduce with an instrument. It may be possible to circumvent the artificial counting of nuclei in the atmosphere by directly sampling the aerosols before entering cloud base, followed up directly with the droplet and ice crystal distribution measurements from a sailplane moving with the updraft. Because of the low cost of sailplanes and sailplane operation it would be feasible to instrument one sailplane to remain just beneath the base of a cloud, monitoring cloud nuclei and other aerosols while another instrumented as above moves with the updraft.

There is considerable justification, based on studies of the mountain wave phenomena in previous years and our own work with the cloud physics sailplane in and around mountain wave clouds, to consider mountain wave clouds as outdoor cloud physics laboratories. The relatively steady state nature of these clouds, forming on the upwind side, growing and then dissipating on the downwind side, provides us with all the basic microphysical data that we could desire on details of the initial microphysical processes for the immediate future. A sailplane can maneuver from one

position to another determined in real time, e.g., crest to trough in the standing wave, sensing the temperature, humidity, vertical motion and microphysical data continuously; or hover at one point while another sailplane is making the aerosol samples up- and downwind of the cloud without either craft perturbing or polluting the cloud itself with engine exhaust or heat. Observations of this type have been made with The Explorer sailplane and have proven its ability to hover in a particular portion of the wave, maneuver for many hours (no fuel required), and seek out features of the cloud of particular interest for research. These mountain wave clouds have proven themselves as valuable outdoor laboratories.

A considerable amount of effort has gone into theoretical calculations and observations of the collision efficiency (probability),  $E_c$ , and some into the accretion efficiency (probability),  $E_a$ . These two quantities are difficult, if not impossible, to measure in natural clouds. Most of our information on the collision efficiency, as it is most commonly termed, comes from theoretical calculations with but a few experimental checks. The information on the accretion (coalescence) efficiency comes almost entirely from a few experimental studies, usually in a very restricted size range.

Davis and Sartor [10] have calculated the hydrodynamic collision efficiencies for cloud drops less than  $30 \mu\text{m}$ . Estimates of the hydrodynamic collision efficiencies of larger drops have been made according to the scheme of Table 2.

Collision efficiencies are calculated for the drop-pair desired by the step-by-step integration of the relative motion of the two drops to obtain their relative trajectories. A hunt and search routine is started when the two drops are a great distance apart to obtain the trajectory that just causes a grazing collision between them. The initial horizontal offset for the critical grazing trajectory, normalized by dividing by the sum of the radii of the two drops, is the "linear collision efficiency". The physically meaningful "collision efficiency" is the square of this term and is assumed to accurately represent the probability of collision when the smaller drop is in the geometrical "collision" zone.

The results of the calculations of hydrodynamic collision efficiencies do not always agree satisfactorily with observations, except in the large drop-size range. Having obtained the hydrodynamic forces and inertial forces on a pair of cloud particles with classical techniques, we add electrostatic forces at each integration step to compute collision efficiencies and to evaluate their total effect on the growth of precipitation and hail in mature thunderstorms, or the growth of electrification from the same processes.

Table 2. Hydrodynamic methods used for calculation of drag forces on cloud drops, raindrops and hail

Radius range [ $\mu\text{m}$ ]		Method used	
$R$	$r$	$R$	$r$
$\leq 50$	$\leq 50$	Two-body Stokes viscous flow solutions from Davis and Sartor [10] calculations	Two-body Stokes viscous flow solutions from Davis and Sartor [10] calculations
$> 50, \leq 100$	$> 50, \leq 100$	McDonald [21] empirical drag calculations in uniform fluid flow	McDonald [21] drag calculations in Stokes (viscous) flow field about $R$
$\geq 500$	All $r$	Beard and Pruppacher [22] drag observations in uniform field flow	Beard and Pruppacher [22] drag observations in potential flow field about $R$



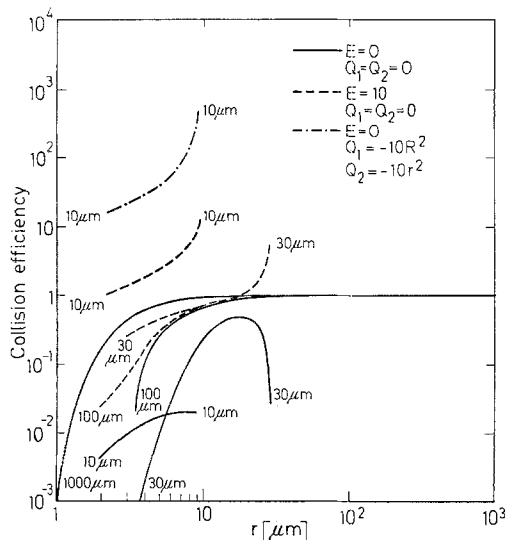


Fig. 4. Collision efficiency versus small drop radius. Curve labels refer to large drop radius in microns and electrostatic parameters [23]

In the absence of electrical forces, the solid line curves of Fig. 4 show that when large drops grow beyond  $100 \mu\text{m}$  radius and the smaller drops increase in radius beyond  $20 \mu\text{m}$ , the collision efficiencies approach unity very closely and tend to remain near that value. The electric fields and charges used in the calculations presented in Fig. 4 are appropriate to mature thunderstorms and have a profound effect on the collision efficiencies, especially when both drops are  $30 \mu\text{m}$  or less. The collision efficiencies of raindrops and hail particles greater than  $1 \text{ mm}$  radius are not greatly affected by electrostatic forces, although in restricted regions of charged drop-size pairings finite differences do exist, they are hardly sufficient to show as separate curves. The rapid drop off as one proceeds from larger to smaller accreted drops below  $4 \mu\text{m}$  can be very significant in preventing a complete sweep out of the cloud; leaving these small drops to grow by condensation as more liquid water is forced out of the rising cloud air by its continued expansion in the strong updrafts of cumulonimbus clouds. According to these calculations, if electrical forces are to play an important role in modifying collision efficiencies, then they must do so when at least some of the drops are quite small but when the charges and/or electric fields are very high. This is not likely very early in the life of a cloud, but the fields and charges in many convective clouds, especially those classified as mature thunderstorms or severe storms, grow very rapidly and remain highly electrified throughout the great majority of their lifetimes. We must remind ourselves at this point, that even in the long lasting, almost "steady-state" thunderstorms, the cloud droplets can grow only by starting out very small, and, in order not to be blown out the top of the storm to shut off further precipitation growth, they must grow very rapidly. The collision efficiencies, alone, do not give a very useful estimate of the total effect of the factors involved in cloud droplet growth. The size distribution, concentration, and relative velocities of the charged cloud particles in an electric field must be accounted for in the calculations involving accretion growth in thunderstorms.

If the drop distribution is held fixed in time while the collision efficiency and relative velocity are allowed to vary with drop size, charge, and electric field, but not with time, the expected instantaneous fractional mass growth rate for selected large spherical particles due to the accretion of smaller drops can be calculated from Eq. (2a) by considering only one large particle at a time,  $n_R = 1$ , and dividing by the mass of the large particle. The inverse cube law is a reasonable choice for the cloud droplet distribution in an accretion process. In the calculations  $E_a$  is taken as unity.

The fields used in these calculations are  $10 \text{ esu}$ , smaller than the observed maximum thunderstorm field by about  $50\%$ , and  $1/10$  that value,  $1 \text{ esu}$ . According to the curves shown in Fig. 5a, the fractional mass growth rate of a  $40 \mu\text{m}$  radius cloud particle changes by an order of magnitude when a field of  $1 \text{ esu}$  is added. The difference becomes 2 or more orders of magnitude if the field is increased to  $10 \text{ esu}$ . The simultaneous addition of charges appropriate to the added field of  $10 \text{ esu}$ , tacks on another order of magnitude or more and does not depend greatly on the orientation of the field with respect to the charges. The effect of charges or fields drops off rapidly with increasing  $R$ , and with increasing  $r$  for each  $R$  selected (see Figs. 5a—d), except at the far right end of the curves where the radius  $r$  approaches  $R$  and where the spread again increases. The increase in the growth rates is most marked when charges and fields are combined. When the accreting particles are less than  $1000 \mu\text{m}$ , the direction of the field does not seem to matter a great deal. Particles of  $1000 \mu\text{m}$  and larger accrete more or less at the non-electrified rate. Depending on the orientation of the charges with respect to the field, differences occur but are not large, typically being generally less than factors of two or three. The difference is due mainly to the difference in terminal velocities of the charged particles in fields of opposite orientation.

The calculations presented in Figs. 5a—d show that typical thunderstorm fields and drop charges drastically change the growth rate of the cloud particles less than  $30 \mu\text{m}$  radius and can affect the growth of precipitation particles greater than  $100 \mu\text{m}$  radius by a factor of two or more. When the precipitation growth process continues and high electric fields and charges are present in a cloud, the electrical forces cannot be ignored. This should be the case in most heavy precipitation storms, and in all mature thunderstorms and severe storms. In many instances the precipitation growth process goes on at an intensity requiring more efficient and faster growth rates for long periods of time after full electrification of the cloud has been attained. For example, the vertical motions shown in the large sheared cumulonimbus model depicted by Newton [11] allow cloud droplets, forming at cloud base, a maximum of seven minutes to grow into precipitation before being carried completely out of the precipitation growth zone. A more realistic estimate might be three or four minutes to agree with radar echo intensity change with height.

It is now clear that the continued precipitation growth process can be greatly accelerated by the appearance of a mature electrical environment of a thunderstorm so that the rapid transition from cloud droplets to precipitation reaches a much enhanced level. Most of

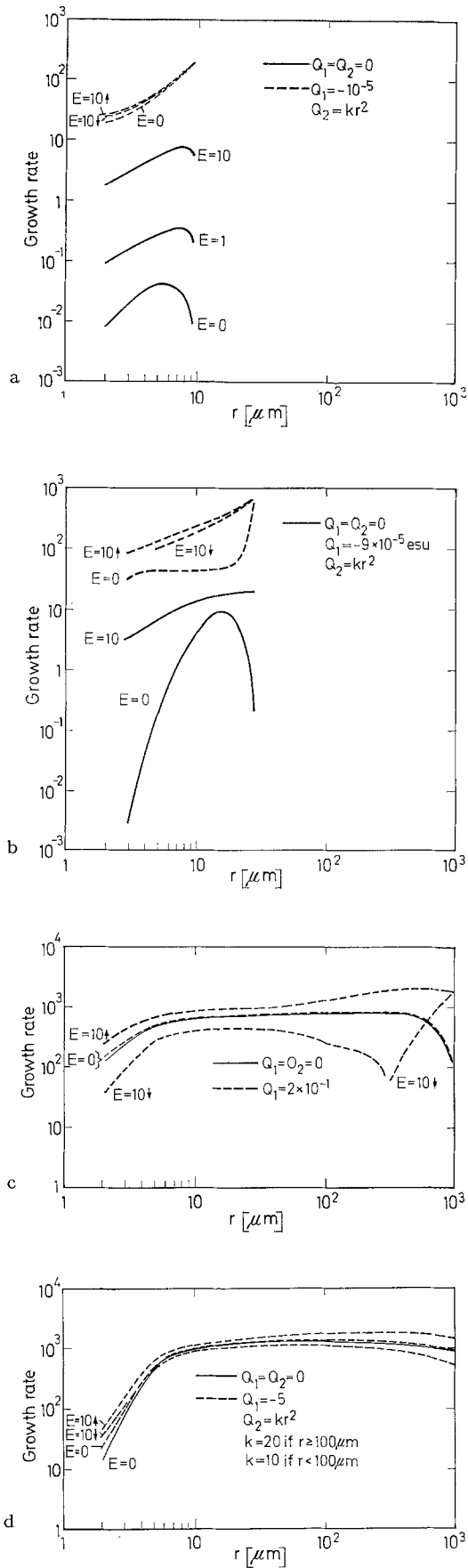


Fig. 5 a—d. Instantaneous mass growth rate of a)  $10\text{-}\mu\text{m}$  drop, b)  $30\text{-}\mu\text{m}$  drop, c)  $1000\text{-}\mu\text{m}$  drop, d) hail embryo with density of 0.6 and radius  $5000\text{-}\mu\text{m}$

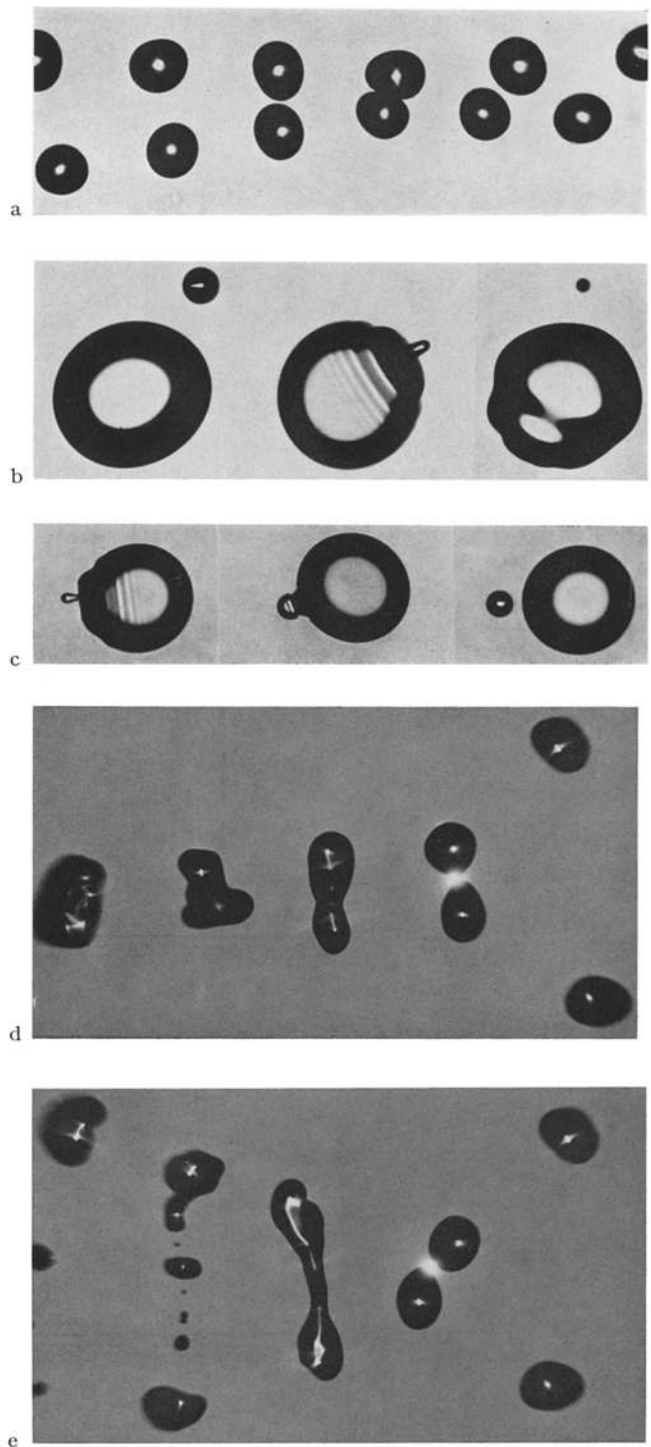


Fig. 6. a)  $390\text{-}\mu\text{m}$  radius bouncing drops in zero ambient field. Charge on each drop is less than  $6 \times 10^{-6}$  esu. Relative velocity is  $30\text{ cm/sec}$  [24]. b) Composite photograph of successive stages of a collision between drops having radii of  $196$  and  $806\text{-}\mu\text{m}$ . The small satellite droplet ejected during coalescence has a radius of  $75\text{-}\mu\text{m}$ . Effective elapsed time between exposures is  $100\text{-}\mu\text{sec}$  [24]. c) Composite photograph of successive stages of a collision between drops having radii of  $196$  and  $806\text{-}\mu\text{m}$ . In this sequence coalescence was complete and satellite drop was not ejected. d) Streams of oppositely charged  $367\text{-}\mu\text{m}$  radius drops on direct collision trajectory. Drop charge is  $74 \times 10^{-12}$  C. Luminous region is a multiple exposure of  $2.6 \times 10^4$  successive discharges between near surfaces. e) Streams of oppositely charged  $367\text{-}\mu\text{m}$  radius drops on grazing collision trajectory. Drop charge is  $74 \times 10^{-12}$  C. Luminous region is a multiple exposure of successive discharges between near surfaces [24].

the time available for precipitation growth is spent in the early stages when all drops are small, and it is among these small droplets that the electrostatic forces are the most effective in speeding up the process. Since the slowest part of the growth process is speeded up the most by the electrostatic forces, it follows that the entire process can be affected significantly, especially since the growth rates of the larger particles, although relatively insensitive to electrostatic forces, increase from one to two orders of magnitude as the smaller drop radius increases from 2 to 20  $\mu\text{m}$  radius. The forces that rapidly increase the growth of the smaller drops among themselves speed up the growth of the larger particles also by providing larger collectable cloud drops more quickly.

Although the accretion probability (efficiency),  $E_a$ , is nearly always taken as unity for coagulation growth computations, it has been known since the previously described experiments of Lord Rayleigh in 1879 to be less than unity for at least a considerable portion of the drop-size range, and for most ice crystals it can be very small. It is now known to be slightly less than unity for collisions between supercooled drops and graupel or other rimed ice particles. It is almost impossible to give reliable values for the accretion probability. The problem is scientifically fascinating since adequate solutions for water drops, especially, will require the judicious trade off of many physical processes which change emphasis with drop size. Examples of some of the types of interactions are illustrated in the photographs in Figs. 6a—e. In Fig. 6a, a series of 390  $\mu\text{m}$  radius drop-pairs "collide", deform and bounce apart. Using weak fields and charges we have determined that no charge is transferred in these collisions and we conclude that the drops were prevented from touching by a layer of air trapped between their near surfaces. Fields of 30  $\text{V cm}^{-1}$  caused coalescence of these drops. Fig. 6b is a composite photo of successive steps in the collision-coalescence of a 806  $\mu\text{m}$  radius drop with a drop of 196  $\mu\text{m}$  radius. Subsequently, in the last position, a drop of 75  $\mu\text{m}$  radius is ejected due to inertial reactions in the fluid of the large drop by the fluid injection of the water from the smaller drop as surface forces and the external inertia of the fluid from the smaller drop react. Fig. 6c depicts a similar event except in this case the coalescence and fluid interaction processes failed to succeed in completing the ejection of a smaller drop. Fig. 6d illustrates successive positions in the complete coalescence of two highly charged 367  $\mu\text{m}$  radius drops. In Fig. 6e, drops of the same size in Fig. 6d collide less directly and the relative momentum of the fluid in each drop, possessing an off-center component, causes subsequent break up and the formation of many smaller drops.

We have also studied the collision and coalescence of much smaller drops, 10 to 100  $\mu\text{m}$  radius. A still air box has been built with a device to produce drops of significantly different size and to place the larger ones behind and above the smaller droplets to observe the interaction for collision and coalescence probabilities under conditions similar to those in a cloud. Fig. 7 is an illustration of the photographs of the trajectories obtained from colliding coalescing drops placed at an initial horizontal offset of many drop radii and given a high charge to produce collision efficiencies affected

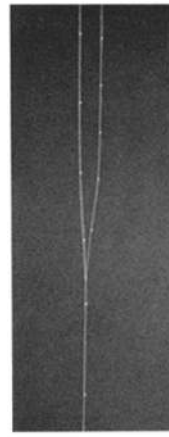


Fig. 7

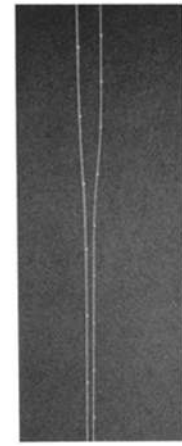


Fig. 8

Fig. 7. Streak photo of a collision between two oppositely charged droplets having radii of 19.1 and 15.6  $\mu\text{m}$  and charges of  $+10.6 \times 10^{-5}$  and  $-6.2 \times 10^{-5}$  esu. Separation of the trajectories at the top of the photo is 685  $\mu\text{m}$ . Bright dots on trajectories are produced by a strobe-light flash every 0.05 sec [25]

Fig. 8. Streak photo of a near miss between two oppositely charged droplets having radii of 19.1 and 15.6  $\mu\text{m}$  and charges of  $+10.6 \times 10^{-5}$  and  $-6.2 \times 10^{-5}$  esu. Separation of the trajectories at the top of the photo is 735  $\mu\text{m}$ . Bright dots on the trajectories are produced by a strobe-light flashing every 0.05 sec

by electrostatic forces. Not all of the data has been worked up for these experiments yet, but the results thus far confirm the high collision efficiencies computed from theory. The drops in Fig. 7 are 19.1 and 15.6  $\mu\text{m}$  radius, respectively, with respective charges of  $+10.6 \times 10^{-5}$  esu and  $-6.2 \times 10^{-5}$  esu. The calculated collision efficiency is 390. In Fig. 8, the drop sizes and charges are the same but the initial horizontal offset is increased by 50  $\mu\text{m}$  and the drops fail to collide. The observed collision efficiencies and trajectories agree with the computer calculations obtained with the procedure described earlier and the coalescence probability is always unity with drops of this size when they are so highly charged.

The collision efficiencies of these droplets without any electrostatic forces or electric fields are so small that the probability of positioning one droplet behind the other so that the collision will result is almost infinitesimal. Also, any very minute movement of the air or electrostatic attraction from outside the chamber causes a serious offset which would result in a non-collision where one might have expected it to occur. However, the collision efficiencies of highly charged drops, being much greater, can be observed this simple way.

In order to obtain collision and coalescence efficiencies of the smaller drops with small charges and electric fields, one must provide an arrangement whereby the larger droplet can be freely suspended and a large number of smaller ones carried upward in a controlled ascending airstream to collide with it. This has been accomplished at the University of California at Los Angeles (UCLA) with a very sophisticated vertical wind tunnel with temperature and humidity control. Studies conducted there have given accurate values of the drag coefficients of small water drops over wide size ranges. By carefully controlling the horizontal profile and velocity of the upward flowing air, one

can control the position of the larger droplet while smaller droplets are being blown upwards in the air-stream to collide with it. Using theoretically calculated collision efficiencies in Eq. (2a) Neiburger, Levin, and Rodrigues [12] deduced the coalescence efficiency from observations of the accumulation of mass on the suspended drop. Whereas something approaching 100% coalescence of colliding drops in the 10–100  $\mu\text{m}$  radius range had been expected, preliminary results of their studies in the UCLA chamber indicated only a 20 to 30% coalescence of some of the droplet pairs. These results, if substantiated by further investigations, place a more important role on smaller charges and electric fields in clouds as they could boost the coalescence considerably. This work can be repeated in a similarly designed vertical wind tunnel at the National Center for Atmospheric Research (NCAR) in which temperature and humidity and turbulence levels can be controlled as in the earlier UCLA tunnel while the electrical environment is controlled also.

The function  $\Psi$  in Eq. (2b) is used to represent any charge transfer mechanism not dependent on the ambient electric field. The main transfer function of this type is due to the thermoelectric charging which occurs when a portion of a cloud or precipitation particle breaks off during freezing or when two colliding particles of different temperatures bounce apart. This charging mechanism results from the different mobilities of charge carriers of opposite sign in ice and water and is usually a function of temperature. Workman and Reynolds [5] were the first to apply thermoelectric charging to cloud electrification processes. These processes have been investigated extensively by Latham and Mason [13], Reynolds, Brook and Gourley [6], and Dye and Hobbs [14]. Pruppacher, Steinberger, and Wang [15] have summarized the work on this problem, finding that the direction and amount of charge transfer is controlled by the type of impurities in cloud water. Although the purest water and the salts most commonly found in rainwater would hypothetically give the correct polarity normally observed in thunderstorms, the function  $\Phi$ , which is a function of the ambient electric field, has been shown by Sartor [16] and Paluch and Sartor [17] to override the charging processes not dependent on the electric field after a short while. This is fortunate since the charge transfer functions resulting from the induction charging of colliding and bouncing cloud particles polarized by the ambient electric field are well known for spherical drops, and can be approximated to a very satisfactory degree for other shapes using the theoretical calculations of Davis [18] and the experimental checks of Sartor and Abbott [3].

Recent laboratory experiments show that under some conditions, induction charge transfer collisions between cloud particles polarized in an electric field (function  $\Phi$ ) that result in bouncing, break up or splattering can be very efficient. The electrical relaxation time for ice at low temperatures is much longer than the contact time of bouncing or separating particles, reducing the amount of charge possible to transfer. Assuming that over some limited temperature range, charge transfer is efficient, the mechanism of polarization charging exhibits some interesting characteristics which agree with a number of observations of cloud electrification.

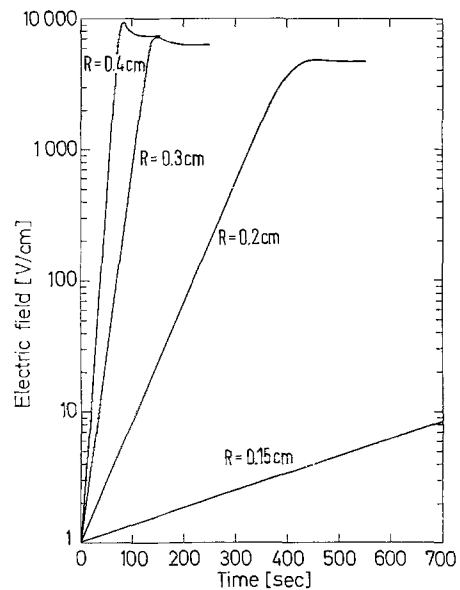


Fig. 9. Electric field strength versus time for different large ice particle radii

The growth of the electric field in clouds can be computed using Eq. (2b) for the charging rate of the particles in a volume of cloud air, and summing the charge over the bottom and top plates of a hypothesized cylindrical volume of large horizontal dimensions. In the computations illustrated in Fig. 9 as the growth of the electric field in a cumulonimbus, Mrs. Paluch and I have considered ice particle collisions only with radii between 0.15 and 0.4 cm. We find similar results for collisions between large ice particles and supercooled cloud droplets, since here the small bounce and splash-off probability is compensated by the presence of large numbers of droplets. We intend to investigate the charge separation in collisions between large ice particles and a mixture of small ice crystals and supercooled droplets in the very near future. This combination of cloud particles should produce the strongest electrification.

The necessary conditions for efficient electrification through ice particle collisions, according to our model, are: 1) the coexistence of precipitation-size particles and small ice crystals (both in relatively high concentrations), 2) cloud temperature sufficiently high (permitting fast electrical relaxation) for polarization charge transfer to be efficient, and 3) a fairly strong updraft (to slow down the passage of the larger charge transfer-efficient particles through the limited fast relaxation zone). These requirements are in agreement with observations by Reynolds and Brook [19] who found that the coexistence of convection and radar-detectable precipitation is a necessary condition for cloud electrification. They are also in agreement with observations by Latham and Stow [20] who measured significant electrification only in regions of the cloud in which rimed aggregates and small ice crystals coexisted, whereas the strongest electric fields were observed when large numbers of supercooled droplets were also present. (Since at temperatures below freezing the number of supercooled droplets as well as the efficiency of polarization charge transfer for ice are expected to increase with increase in cloud

temperature, the presence of strong fields in regions where high concentrations of supercooled droplets exist is compatible with the ice particle polarization charging mechanism.)

The observed complex electric field structures, including reverse fields accompanied by sign reversal of the dominant ice particle charges, can be explained in terms of polarization charging within a spatially limited region in presence of varying updrafts.

The rain gush frequently observed after a lightning discharge is an expected consequence of the electrical forces acting on the charged particle terminal velocities in a direction that tends to accumulate them in regions of strong electric fields.

Since the efficiency of electric field generation due to the spatially limited charging levels has a maximum near  $1/2$  the fall speed of the precipitation-size particles, we expect updrafts of about 4 m/sec or higher in regions where efficient electric field build up takes place. Such updrafts are common only to convective clouds—the only type normally associated with thunderstorms.

Undoubtedly there are a number of charging and discharging mechanisms operating in thunderstorms. However, since this rather simple model does provide coherent explanations of the observed large scale electrical phenomena in thunderstorms, it is possible that polarization charging is an important mechanism for thunderstorm electrification. In fact, it may be that, due to the fundamental nature of the physical

and electrical interactions evoked in these calculations, polarization charging must be considered an integral part of any complete thunderstorm theory.

- [1] Whelpdale, D. M., List, R.: *J. Geophys. Res.* **76**, 2836 (1971). — [2] Montgomery, D. N.: *J. Atmos. Sci.* **28**, 291 (1971). — [3] Sartor, J. D., Abbott, C. E.: *J. des Recherches Atmospheriques (Dessens Memorial Issue)* (in press). — [4] Foote, G. B.: Ph. D. Thesis, University of Arizona, Tucson, Arizona (1971). — [5] Workman, E. J., Reynolds, S. E.: *Phys. Rev.* **78**, 254 (1950). — [6] Reynolds, S. E., Brook, M., Gourley, M. F.: *J. Meteorol.* **14**, 426 (1957). — [7] Jones, R. F.: *Quart. J. Roy. Meteorol. Soc.* **86**, 187 (1960). — [8] Cannon, T. W.: *Image Technol.* **12**, 37 (1970). — [9] Abbott, C. E., Dye, J. E., Sartor, J. D.: *J. Appl. Meteorol.* **11**, 1092 (1972). — [10] Davis, M. H., Sartor, J. D.: *Nature* **215**, 1374 (1967). — [11] Newton, C. W.: *Tellus* **18**, 699 (1966). — [12] Neiburger, M., Levin, Z., Rodriguez, L.: *J. des Recherches Atmospheriques (Dessens Memorial Issue)* (in press). — [13] Latham, J., Mason, B. J.: *Proc. Roy. Soc. A* **260**, 523 (1961). — [14] Dye, J. E., Hobbs, P. V.: *J. Atmos. Sci.* **25**, 82 (1968). — [15] Pruppacher, H. R., Steinberger, E. H., Wang, T. L.: *J. Geophys. Res.* **73**, 574 (1968). — [16] Sartor, J. D.: *Arch. Meteorol. Geophys. Bioklimatol.*, (A) **21**, 273 (1972). — [17] Paluch, I. R., Sartor, J. D.: *J. Atmos. Sci.* (in press). — [18] Davis, M. H.: *Quart. J. Mech. Appl. Math.* **17**, 499 (1964). — [19] Reynolds, S. E., Brook, M.: *J. Meteorol.* **13**, 376 (1956). — [20] Latham, J., Stow, C. D.: *Quart. J. Roy. Meteorol. Soc.* **95**, 486 (1969). — [21] McDonald, J. E.: *J. Meteorol.* **17**, 463 (1960). — [22] Beard, K. V., Pruppacher, H. R.: *J. Atmos. Sci.* **26**, 1066 (1969). — [23] Sartor, J. D.: *J. Geophys. Res.* **75**, 7547 (1970). — [24] Sartor, J. D.: *Physics Today* **22**, 45 (1969). — [25] Sartor, J. D.: *ibid.* **25**, 32 (1972).

Received June 26, 1972